OPTIMIZATION DESIGN OF POWER SYSTEM TRANSFORMATION FOR AIR UNMANNED HELICOPTER

He LI[1], Yahui ZHANG, Ali Tahir SHAHID, Shuai LIU *

In order to improve aerodynamic system of unmanned aerial helicopter platform, several characteristic analysis are necessary to be done mainly on engine, installation, transmission, cooling & exhaust pipe of MZ202 & Rotax582. Specifically for Rotax582 retrofit design of standard engine. This article describes the main problems and its reliable solutions in optimization design process. Similarly, strength check & modal analysis for key part design are carried out via Ansys and finite element modeling prior to test verifications. The results have shown that this method is feasible. The datasets which were collected by flight control system showed that, rotation speed fluctuates around 20 rpm. After conversion to engine speed the fluctuations were in the scope of -50 and 50 rpm, indicating stability in rotational speed. The exhaust pipe temperature recorded 6oC, the engine cylinder temperature recorded 100°C and coolant temperature was at 80°C. The engine vibration level is 0.05g and there are no abnormalities found in data. These datasets are helpful in further optimization of engine systems for light weight air helicopters and could serve as potential reference material for fixing errors during transformation of power systems.

Keywords: Unmanned helicopter, Power systems, Optimal design, Strength analysis, Modal analysis

1. Introduction

Unmanned aerial helicopter has variety of application prospects due to its properties such as vertical takeoff and landing, fixed point hover and lowering speed at lower altitudes [1, 2]. Rotor system is driven by the mechanical energy obtained from the fuel [3]. Performance is determined by the extent of control during constant engine speed [4-6]. Mainly, engine powers the aerodynamics of the blades to provide lift during flight thus engine plays the critical role in use of helicopter and known as the brain of helicopter [7]. Commercially, there are three kinds of power systems used in unmanned helicopter, piston engine, turbo-shaft engine and rotor engine. To reduce the weight of machine piston engine is more commonly recommended [8]. This study evaluates and concludes the best power system for light unmanned aerial machines.

[1] College of Mechanical and Electrical Engineering, Henan Agricultural University, Zhengzhou 450002, China
*Corresponding author: 674407361@qq.com

Swing clutch is utilized to switch on and off engine and rotor rotation. It is also responsible for the stability during flight. Amount of output torque and speed of engine should certainly have that range of stability to ensure successful air maneuverability. Through investigation of domestic and foreign aviation engines it was decided that Rotax series engines for example MZ202, Intec800 etc. are best suited for light weight unmanned aerial helicopter [9-12]. Among them Rotax582 was chosen to have best match for 180kg single rotor helicopter. The design was tested under variant test environments for possible error and their solutions.

2. Materials and Methods

Comparison of Engine Characteristic Curves

The study showed that, idle speed of standard Rotax582 engine can be adjusted to 1600rpm, which is lower than combined speed of the swing clutch at 2200rpm. However, according to the torque characteristic curves of both engines, at the stage from 6000rpm to 6500rpm, the Rotax582 standard model decreased at the rate of 9NM and MZ202 at the rate of 5NM, indicating that the Rotax582 standard model decreased more smoothly than the MZ202, and the throttle was more responsive and showed better maneuvers (Fig. 1). In terms of the helicopter's load capacity and flight speed, the direct influence factor is power of the engine. By contrast, MZ202 is air-cooled cooling, while Rotax582 standard type is water-cooled cooling. The cooling effect will be better than MZ202 to ensure the engine has a good working environment. [13-15].

Seat Installation Design and Check

Because the Rotax582 standard two carburetors are float carburetors, they must be installed vertically. When the engine is installed vertically, the two carburetors cannot be installed vertically on the original basis due to the space limitation, so the rubber sleeve needs to be redesigned. The basic requirement is to ensure that there is enough space for the two carburetors to be installed vertically, and the two do not interfere in the operation of the engine. The two carburetors and the cylinder block are connected vertically by the elbow rubber sleeve and clamp. Namely, the upper carburetor is installed vertically to the left, and the lower carburetor is installed vertically to the right.

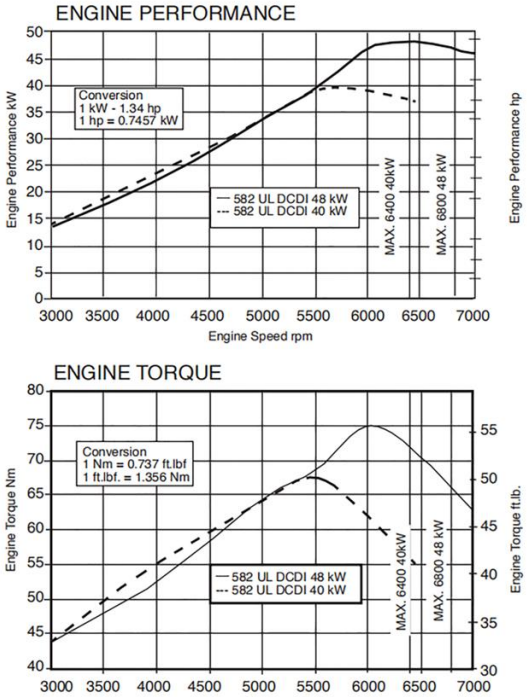

Fig. 1. Working condition diagram of Rotax582 engine

On the structure of the existing AIR unmanned helicopter body, the mounting hole used by the MZ202 engine is used to install the Rotax582 engine, and the upper mounting seat and the lower mounting seat need to be designed. Design key points have the following three aspects, first, fully let the rubber shock absorption column half connected to the body support, the other half connected to the mounting seat, its purpose is to ensure that the engine has good shock absorption. Secondly, due to assembly and machining errors the longitudinal distance between the shaft and the engine should be adjustable. The method is to adjust the longitudinal distance by adding adjustment gaskets between the engine and the transfer seat through actual assembly. In other words, the mounting seat should be smaller in the longitudinal height. Again, for ease of installation the upper mounting seat hole is a round hole, and the lower mounting seat hole is a slot hole. Thirdly, in the upper end of the top transfer seat, it is necessary to design the pretightening structure to adjust the tension force of the belt pulley.

By using finite element software of engine installation for structural static strength analysis, the static analysis was carried out on the installation seat before the applied load. Finite element model is based on simplified load and boundary conditions [16,17]. The load input is inertia force of engine 38.3kg, the maximum force of mounting seat is 7.99mpa. According to material data, the yield strength of mounting seat is 455Mpa (Fig. 2).

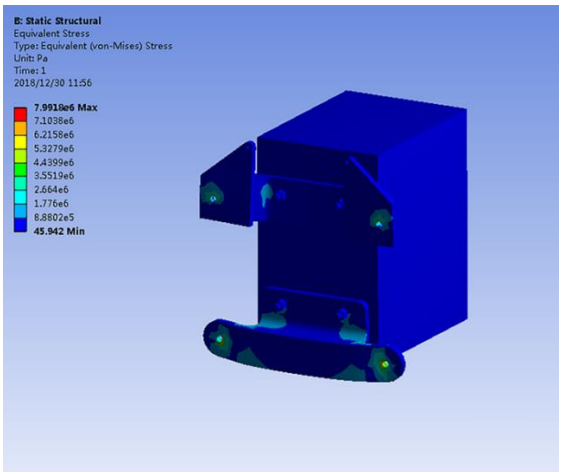

Fig. 2. Engine mounting seat design

Engine Installation Method

The installation method recommended by the Rotax582 engine manufacturer is horizontal installation, but the horizontal installation method based on the AIR unmanned helicopter platform will bring additional retrofit design, which requires the addition of a transmission reducer, resulting in increased weight of the helicopter itself and reduced transmission efficiency. Extend project cycle, etc. If the installation is vertical, the carburetor needs to be modified, that is, the installation of carburetor must also be vertical. After the comprehensive evaluation, the engine body is vertically mounted, which is connected to the aircraft body by transfer plate and connected by rubber-metal vibration absorber column, thus reducing the transmission of engine vibration to the aircraft body (Fig. 3).

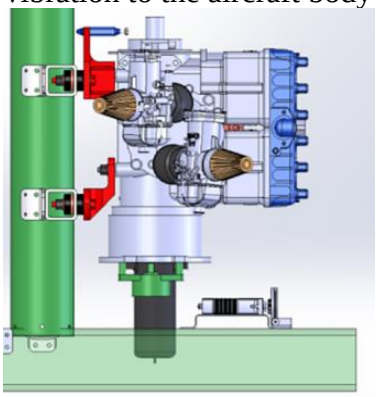

Fig. 3. Engine installation drawings

Propagation of engine vibration directly affects the reliability and service life of the whole machine, so some effective measures must be taken to reduce vibrations [18,19]. The interference force of the engine itself is the vibration source of

active vibration isolation. Dynamic load transferred to engine body is equal to maximum value of the interference force, expressed by *eq.* 3. If there is a rubber-metal shock absorber between engine and engine body, the forced vibration equation of engine will be as:

$$\chi = B\sin(\omega t + \varphi) \tag{1}$$

It's amplitude B is:

$$B = \frac{B_0}{\sqrt{(1-\lambda^2)^2 + 4\zeta^2\lambda^2}} \tag{2}$$

At this time, the dynamic load transferred from the engine to the engine body through the rubber-metal shock absorber column is:

$$F_N = F_k + F_C + \mu\dot{\chi} \tag{3}$$

$$F_N = kB\sin(\omega t - \varphi) + cB\omega\cos(\omega t - \varphi) \tag{4}$$

$$\sqrt{(kB)^2 + (cB\omega)^2}\cos\theta = \mu B\omega\sqrt{(kB)^2 + (cB\omega)^2}\sin\theta$$

Note:

k represents the rigidity coefficient of rubber-metal vibration absorber column

c represents the damping coefficient of rubber-metal damping column

Then the dynamic load can be expressed as:

$$F_N = \sqrt{(kB)^2 + (cB\omega)^2}\sin(\omega t - \varphi + \theta) \tag{5}$$

At this point, the interference force by passive vibration isolation of the engine is:

$$F = m\ddot{\chi}_1 = -mr\omega^2\sin\omega t \tag{6}$$

Note: *m* depicts engine payload

Under above conditions, the ratio *k* of the maximum dynamic load transferred from the engine to the engine body is defined, where *k* is called the vibration isolation coefficient. Therefore, it can be obtained as follows:

$$K = \frac{F_{N\max}}{F_0} = \frac{\sqrt{(kB)^2 + (cB\omega)^2}}{F_0} = \frac{kB\sqrt{1+(\frac{c\omega}{k})^2}}{F_0} \tag{7}$$

Because:

$$\frac{F_0}{k} = B_0 \qquad \frac{c\omega}{k} = \frac{c\omega}{m\omega_n^2} = 2\frac{n}{\omega_n}\times\frac{\omega}{\omega_n} = 2\zeta\lambda$$

The above formula can be written as:

$$K = \frac{\sqrt{1+4\zeta^2\lambda^2}}{\sqrt{(1-\lambda^2)^2 + 4\zeta^2\lambda^2}} \tag{8}$$

When the zeta = 0, based on the relationship between K, frequency and lambda will be as:

$$K = \left|\frac{1}{1-\lambda^2}\right| \tag{9}$$

Damping ratio can also be calculated from isolation coefficient and frequency relationship curve [20-22].

Two conclusions can be drawn from the analysis:

1) Irrespective of the damping value, as long as the isolation coefficient K < 1, a better effect of vibration reduction can be obtained. Therefore, the rubber shock absorber with lower rigidity should be used. The greater the frequency ratio of lambda the better would be the isolation, which is generally 2.5-5.

2) To reduce the maximum vibration amplitude of the engine in the resonance region, it can be achieved by increasing the damping ratio. However, at > 2, even if the vibration coefficient K increases, the isolation effect decreases. So the damping ratio is generally selected values of zeta, 0.02 to 0.1.

The rubber-metal shock absorber column is made of two elastomers bonded to a central steel tube, internally reinforced with a cylinder of 30CrMnSiA steel. The elastomer was selected from chlorobutadiene. Choose zeta damping ratio= 0.2, frequency selection than lambda 3.5, both with strong rigidity, and can play a good damping effect. The steel tube diameter of 12mm, wall thickness of 1.25mm and length of 33mm were preliminarily determined. Then the finite element software was used to calculate the maximum stress of 30CrMnSiA steel tube, which was 49.3mpa, while the yield strength of the material 30CrMnSiA was 875Mpa, so the static strength met the design requirements (Fig. 4).

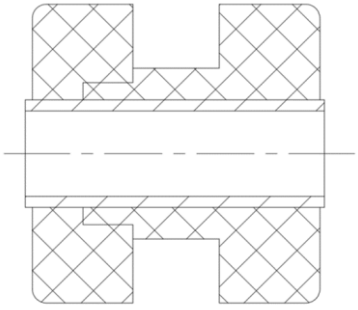

Fig. 4. Rubber metal shock absorber design

3. Engine Accessories

Cooling System Design

The water tank is a key component in the engine cooling system, whose function is to force liquid cooling on the engine to keep the engine performance stable [23-25]. The maximum coolant temperature rise for the engine is 80-130 degree Celsius. The theoretical calculation formula of the radiator tank is as following:

$$Q = k_1 A \Delta T \tag{10}$$

Note:

Q represents the heat loss of the radiator

k represents the heat dissipation coefficient of the radiator

A represents the area of the radiator

T represents the temperature difference between gas and liquid
Calculation of fan volume is as following:

$$G = k_2 d_m^3 n \tag{11}$$

Note:
G stands for fan volume
k represents proportional coefficient
d Represents fan diameter
n stands for fan speed

The factors that determine cooling effect of water tank generally include effective cooling area, central part of the radiator air flow and flow rate of cooling tube coolant. According to the test results, the coolant flow rate increased from 0.2m/s to 0.8m/s, and the cooling effect increased rapidly, but after exceeding 0.8m/s, the cooling effect was stagnant [26].

The radiator tank tilts 30° and is installed in front of the body. For engine cooling system, waterway design is crucial to ensure that the engine cooling system has good water circulation conditions (Fig. 5). The coolant passes through an internal waterway, carries some heat from the engine, and exits from the other side of the engine to the water tank to complete the coolant circulation. At the same time, the cylinder head exhaust pipe needs to be connected to the water injection port in order to adjust the internal pressure of the engine [25-27].

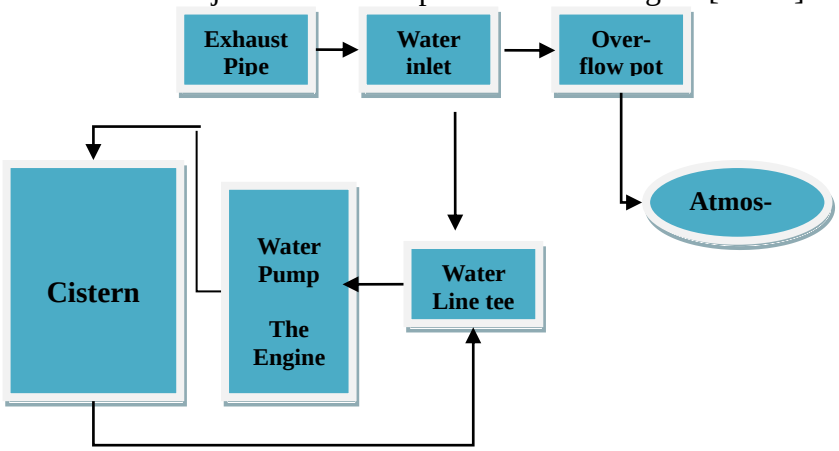

Fig. 5. Refrigerating system layout

Vibration Analysis of Mounting Bracket

Engine operation and rotor operation are the periodic simple harmonic vibration, generated by the helicopter and are the two main vibration sources causing the helicopter body to shake [28]. If the natural frequency of mounting bracket is equal to or close to excitation frequency of engine or rotor, then the body and

mounting bracket will produce resonance phenomenon, so vibration analysis of mounting bracket must be carried out.

The structure of UAV helicopter body is a multi-degree-of-freedom elastic structure, and the mounting bracket is only a subset of the structure, so the mounting bracket is also a multi-degree-of-freedom elastic structure. According to the characteristics of the system, the frequency equation is established as follows:

$$(K - \omega^2 M)u = 0 \tag{12}$$

These equations are value problems for matrices M and K. Where u is a constant and a non-zero solution exists if and only if the determinant of the coefficients is equal to zero. That is:

$$\Delta(\omega^2) = \det(K - \omega^2 M) = 0 \tag{13}$$

After expanding the above equation, the n degree algebraic equation can be obtained:

$$\omega^{2n} + a_1\omega^{2(n-1)} + a_2\omega^{2(n-2)} + \ldots + a_{n-1}\omega^2 + a_n = 0 \tag{14}$$

This n^{th} algebraic equation has n roots (r=1, 2... N), these roots are called eigenvalues,

They are called the natural frequencies of the system.

The natural frequency (r=1, 2... N) When substituted into the equation respectively to obtain:

$$(K - \omega_r^2 M)u^{|r|} = 0 (r = 1,2,\ldots,n) \tag{15}$$

When the eigenvalues are solved, the non-zero solution vector can be obtained. The vector is called the eigenvector of the corresponding eigenvalue, also known as the mode vector which represents the natural mode of the system [29].

By inquiring relevant parameters of the AIR unmanned helicopter, the main rotor speed is 540r/min and the tail rotor speed is 2450r/min.

While the normal engine speeds range is 1600-6500r/min. According to the formula:

$$f = \frac{n}{60} \tag{16}$$

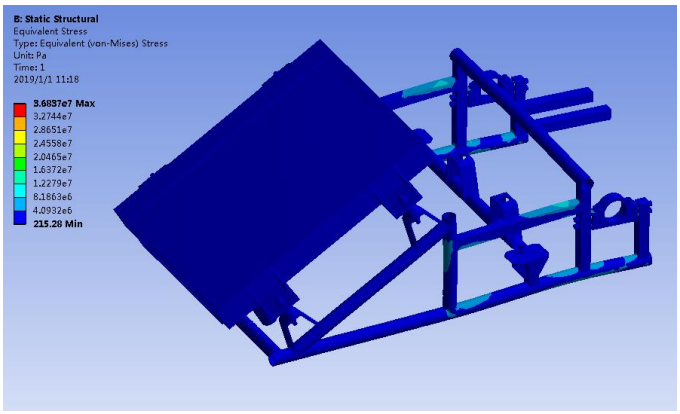

Fig. 6. Mounting bracket design

The available engine excitation frequency range is 26.6Hz-108.3Hz, main rotor excitation frequency range is 0Hz-9.6Hz, tail rotor excitation frequency range is 0Hz-40Hz. ANSYS finite element software was used to evaluate the 10th mode of the mounting bracket, and the natural frequency and mode shape of the 6th mode were analyzed, as shown in (Fig. 6 & Fig. 7).

Mode	Frequency [Hz]
1.	29.499
2.	37.85
3.	74.621
4.	163.65
5.	217.77
6.	220.02
7.	244.91
8.	254.29
9.	270.
10.	335.47

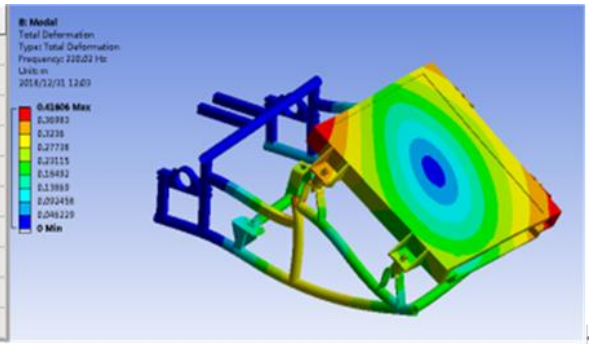

Fig. 7. Modal analysis of mounting bracket

By analyzing, the mounting bracket is mainly affected by the engine driving frequency. According to the data analysis, the engine idle frequency is 26Hz, and the 1st vibration frequency of mounting bracket is 29.5Hz (Fig. 7), which can be realized by adjusting the engine idle speed. On one hand, the natural frequency to avoid the engine mounting bracket work incentive frequency range, the unmanned helicopter flight speed 6000 r/min, the corresponding Rotax582 standard engine has frequency of 100 Hz, and the mounting bracket 4 order natural frequency of 163.35 Hz, 5 order natural frequency is 217 Hz (Fig. 7), therefore, during unmanned helicopter's flight, it won't produce resonance. Finally, the engine excitation frequency corresponding to the natural frequency of mounting bracket should be passed quickly (Table 1).

Table 1

Experimental Verification of Mounting Bracket

Order time	Test frequency （Hz）	Excitation Frequency （Hz）	Error (%)
1	28.65	29.499	2.88
2	39.26	37.85	3.73
3	78.62	74.621	5.36
4	150.36	163.65	8.12
5	216.6	217.77	0.54
6	229.37	220.02	4.25

4. Analysis and Discussion

Test Verification

After optimized design and structural assembly of standard engine of Rotax582 are completed (Fig. 8), the mounting bracket modal test is solved at the engine test stage [2]. The experimental data of modal test were compared with the analysis data to verify the accuracy of the analysis data.

$$ER(f_i^a, f_i^x) = \frac{|f_i^a - f_i^x|}{f_i^a} \tag{17}$$

ER is the error of modal frequency (Hz)

Fig. 8. Customized structural design of unmanned aerial helicopter

Next, electrical connection to the engine was made and following systems were tested: cooling system, fuel system, start system, ignition system and lubricating oil system. After confirming the correctness, constant speed test for the engine was done. The second group of fixed speed was about 20min. By analyzing the data collection controlled by the flight control system, the speed data fluctuated around ±20rpm, which was converted into the engine speed and around ±50rpm. The speed stability was good. The exhaust pipe temperature was 600, the engine cylinder temperature is 100, and the coolant temperature is 80, with no ab-

normal data. The vibration level of the engine is 0.05g, and the mounting bracket has no resonance and low noise.

5. Conclusions

This article is a theoretical detailed analysis of the AIR unmanned helicopter platform, the Rotax582 standard engine system is modified and optimized for this purpose, and the general idea of the transformation of the unmanned helicopter power system is discussed, providing a theoretical basis for production and manufacturing. The following conclusions are drawn:

(1) Vertical installation is adopted for the engine body, which is connected to the aircraft body by transfer plate and connected by rubber-metal vibration absorber column, thus reducing the transmission of engine vibration to the aircraft body.

(2) Finite element software was used to analyze the structural static strength of the engine mounting seat. According to the analysis results, the maximum force on the mounting seat was 7.99Mpa. According to the material data, the yield strength of the mounting seat was 455Mpa, which met the design requirements.

(3) For the i-axis material, Al7075-t6 is selected, and the allowable shear stress for torsion is 303Mpa, and 3 is taken as the safety factor. The maximum allowable shear stress of i-axis is 101MApa. The outer diameter of the shaft is 30mm and the inner diameter is 20mm. It is concluded that the shear stress of i-axis is 17.6Mpa, falls in the safety range.

(4) After modification of the power system of the AIR unmanned helicopter, the ground test and test flight results showed that the optimized UAV power system has good rotational speed stability, no resonance in the mounting bracket, and low noise.

Acknowledgements

This research was supported by ‘thirteenth five-year’ specific grant funded by China Agriculture Research System (Grant No. CARS-04-PS25); National Key R&D Plans, Corn Mechanization Production Technology Integration Demonstration (2018YFD0300704). Furthermore, authors would sincerely thank reviewers for their very professional suggestions on this study.

REFERENCES

[1]. *Z. Guo-gui, L. Zhilin and K. Zhao-cheng.* “Design and test of speed control of piston electro-jet engine for a certain unmanned helicopter”, Journal of aeronautical dynamics, **vol. 26, no. 06,** 2011, pp. 1384-1388.

[2]. *J. Downs, R. Prentice, S. Dalzell and A. Besachio.* “Control system development and flight test experience with the MQ-8B fire scout vertical take-off unmanned aerial vehicle (VTUAV)”, AIAA. American Helicopter Society 63rd Annual Forum, Virginia, USA, 2007, pp. 322-340.

[3]. *B. A. Haider, C. H. Sohn, Y. S. Won and Y. M. Koo.* “Aerodynamically efficient rotor design for hovering agricultural unmanned helicopter”, Journal of Applied Fluid Mechanics, **vol. 10**, 2017.

[4]. *B. Q. Song, J. K. Mills, Y. H. Liu and C. Z. Fan.* “Nonlinear dynamic modeling and control of a small-scale helicopter”, International Journal of Control, Automation and Systems, **vol. 8**, 2010, pp. 534-543.

[5]. *I. M. Yassin, M. N. Taib and R. Adnan.* "Recent advancements & methodologies in system identification: A review", Scientific Research Journal, **vol. 1**, 2013, pp. 14-33.
[6]. *F. Yacef, O. Bouhali, M. Hamerlain and N. Rizoug.* "Observer-based adaptive fuzzy backstepping tracking control of quadrotor unmanned aerial vehicle powered by li-ion battery", Journal of Intelligent & Robotic Systems, **vol. 84, no. 1,** 2016, pp. 179-197.
[7]. *Z. Tenghao*. "Torsional vibration analysis and optimization of automotive power transmission system", Nanjing: nanjing university of aeronautics and astronautics, 2013. (in Chinese)
[8]. *W. Xiaoqing, H. Yimin and Y. Yidong*. "Control strategy of piston electronic injection engine in small unmanned helicopter", Acta aero sinica, **vol. 8**, 2015, pp. 928-932 (in Chinese).
[9]. *X. Ming and L. Zekun.* "New characteristics of European unmanned helicopter research and development", Aviation science and technology, **vol. 8**, 2015, pp. 6-9 (in Chinese).
[10]. *M. B. Tischler and R. K. Remple.* "Aircraft and rotorcraft system identification: Engineering", Scientific Research Journal, **vol. 1**, 2013, pp. 14-33.
[11]. *B. A. Haider, C. H. Sohn, Y. S. Won and Y. M. Koo.* "Aerodynamically efficient rotor design for hovering agricultural unmanned helicopter", Journal of Applied Fluid Mechanics, **vol. 10**, 2017.
[12]. *Z. Peijun*. "Analysis of several common faults of motorcycle idle system", Motorcycle technology, **vol. 8**, 2016, pp. 68-71 (in Chinese).
[13]. *S. Tang, Z. Q. Zheng, S. K. Qian and X. Y. Zhao*. "Nonlinear system identification of a small unmanned helicopter", Control Engineering Practice, **vol. 25**, 2014, pp. 50-63.
[14]. *X. S. Lei and Y. H. Du.* "A linear domain system identification for small unmanned aerial rotorcraft based on adaptive genetic algorithm", Journal of Bionic Engineering, **vol. 7**, 2010, pp. 142-149.
[15]. *T. Y. Jiang, L. Ji and K. W. Huang.* "Longitudinal parameter identification of a small unmanned aerial vehicle based on modified particle swarm optimization", Chinese Journal of Aeronautics, **vol. 28**, 2015, pp. 865-873.
[16]. *I. B. Tijani, R. Akmeliawati, A. Legowo and A. Budiyono.* "Nonlinear identification of a small scale unmanned helicopter using optimized NARX network with multiobjective differential evolution", Engineering Applications of Artificial Intelligence, **vol. 33**, 2014, pp. 99-115.
[17]. *L. Yongbiao*. "Research on dynamic model of engine vibration isolation system based on magnetorheological change", Chongqing: chongqing jiaotong university, 2008. (in Chinese)
[18]. *Z. Longgang, D. Yongbo, W. Junliang and L. Wei.* "Discussion on vibration isolation technology of engineering machinery engine", Internal combustion engine, **vol. 2**, 2013, pp. 38- 40,43 (in Chinese).
[19]. *S. Yan and H. Zuiting.* "Theoretical mechanics of planning textbooks for colleges and universities in the 21st century", China electric power press, 2006, pp. 252-253 (in Chinese).
[20]. *X. Ding.* "Improvement of protection performance of starting motor of micro car", Equipment manufacturing technology, **vol. 8,** 2015, pp. 136-137 (in Chinese).
[21]. *X. Hui.* "Research on matching of WD615.46 vehicle diesel engine", Tianjin: tianjin university, 2007. (in Chinese)
[22]. *G. Changbin.* "Influence of glass fiber on rubber oil corrosion resistance", Corrosion science and protection technology, **vol. 4,** 2005, pp. 252-254 (in Chinese).
[23]. *Z. Shiyi.* "Research on performance of dual-clutch automatic transmission system", Chongqing: chongqing university, 2008. (in Chinese)
[24]. *C. Yinlong.* "Calibration and matching of electronic thermostat", Shenyang: shenyang university of technology, 2014. (in Chinese)
[25]. *Z. Zhiguo.* "Research on optimization of motorcycle water cooling system", Tianjin: tianjin university, 2011. (in Chinese)
[26]. Ansys Fluent Release 18.2, ANSYS® Academic Research, Help System, "Fluent Theory and User's Guide" ANSYS Inc. 2018.
[27]. *N. Jia.* "Research on the modeling and optimization of helicopter body dynamics based on finite element method", Nanjing: Nanjing university of aeronautics and astronautics, 2013. (in Chinese)
[28]. *F. Chen.* "Application of eigenvalues and eigenvectors of matrices", Future talent, **vol. 23**, 2015, pp. 239 (in Chinese)
[29]. methods with flight-test examples, Journal of Guidance, Control, and Dynamics, **vol. 36**, 2013, pp. 1249-1250